JACS
JOURNAL OF THE AMERICAN CHEMICAL SOCIETY

COMMUNICATION

pubs.acs.org/JACS

On the Circular Birefringence of Polycrystalline Polymers: Polylactide

Hai-Mu Ye,[†] Jun Xu,*[,†] John Freudenthal,[‡] and Bart Kahr*[,‡]

[†]Department of Chemical Engineering, Tsinghua University, Beijing 100084, China

[‡]Department of Chemistry, New York University, 100 Washington Square East, New York, New York 10003, United States

Supporting Information

ABSTRACT: The circular birefringence of polycrystalline polymers is invariably obscured by strong linear birefringence. To parse the two mechanisms of light retardation, polycrystalline spherulites of polylactide enantiomers were analyzed by Mueller matrix microscopy. Polymer films are barely optically active in normal incidence, but if illuminated obliquely they become strongly optically active. Opposite hemispheres have oppositely signed circular birefringence. The sign is independent of the enantiomer but dependent on the sense of the sample's tilt. These observations are consistent with light path inhomogeneities resulting from stacked, mis-oriented lamellae. Chiroptical commonalities based on symmetry arguments are discussed among polylactide, a single oriented water molecule, and microfabricated metamaterial arrays, as well as the first physical model of optical activity, Reusch's pile of mica plates. The latter model provides the best explanation of the circular birefringence of polylactide spherulites. The only data on the optical rotation of crystalline polymers to date come from ostensible single crystals of polylactide. The enormous, anisotropic optical rotations observed previously are in quantitative agreement with misoriented lamellae observed here. Limitations of parsing circularly birefringent systems into those showing 'natural optical activity' and those others, somehow 'unnatural', are discussed.

Polymers built from chiral monomers can manifest their local dissymmetry in extended chain conformations, packing of chains in lamellae, and the packing of lamellae into polycrystalline ensembles. Researchers refer to these organizational length scales as 'levels of chirality' and make attractive analogies to the primary, secondary, tertiary, and quaternary structures of proteins.[1] It is natural to imagine that the interactions of such hierarchical chiral systems with circularly polarized light might yield structural insights. While the chiroptical responses of polymers of enantioenriched monomers in helical conformations have been well studied for molecules in solution,[2] we are ignorant of the chiroptics of lamellar organization on the mesoscale. This is because linear anisotropies invariably mask changes to circular polarization states in solids. It was our aim, here, to evaluate the higher order chiroptical consequences of polycrystallinity in chiral polymers. To do so it was necessary to bring new methods of analysis to bear on the problem of proliferating chirality length scales.

Herein, we describe the application of Mueller matrix microscopy (MM)[3] to the analysis of the linear birefringence (LB) and circular birefringence (CB) of polylactide (PLA) spherulites.

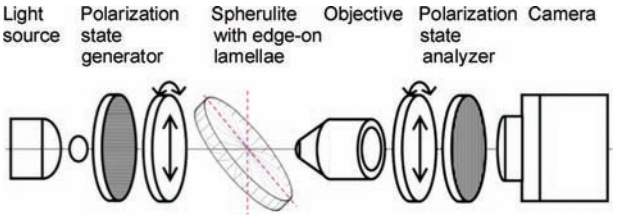

Figure 1. General experimental configuration for examination of spherulites with Mueller matrix microscope. The polarization state generator and analyzer are made from fixed linear polarizers and rotating wave plates.

PLA[4] is an environmentally benign bioplastic[5] made from renewable resources. Its crystallization determines the properties of items that can be fabricated from it. MM analyzes the linear optical properties of a complex sample through a matrix of images, the so-called Mueller matrix (M),[6] the linear operator that describes the transformation of the input Stokes vector (S_{in}) describing the polarization state of the instrument-generated light, to the output Stokes vector (S_{out}) generated after interaction by the sample: $S_{out} = MS_{in}$. The sixteen raw images of M are not simply related to fundamental optical constants including CB and LB.[7] To isolate these quantities, we carried out an analytical decomposition of the raw M.[8] Mueller matrix imaging is well suited to the optical analyses of complex chemical systems.[9] Figure 1 shows the arrangement of the sample with respect to the microscope optical path.

Semicrystalline PLA enantiomers, poly(L-lactide) (PLLA) and poly(D-lactide) (PDLA), are commercially available.[10] PLA crystallizes in the enantiomorphous, orthorhombic space group $P2_12_12_1$ with a = 10.66(1) Å, b = 6.16(1) Å, and c (chain axis) = 28.88(2) Å.[11] The morphology of PLA spherulites is varied and has been studied by many research groups using an array of analytical methods.[12] Invariant, however, is the radial b-axis. Either a or c can project perpendicular to the substrate. It was shown that the optically negative spherulites (Figure 2a,b) are made up of edge-on lamellae with tangential chains, while the optically positive (Figure 2c) spherulites are made up of flat-on lamellae with chains perpendicular to the substrate. The negative spherulites of PDLA and PLLA were obtained from the melt at 120 °C, and the positive PDLA spherulites were obtained at 150 °C.[13]

Figure 2d–f show the |LB| micrographs (λ = 630 nm) of negative PDLA and PLLA spherulites and a positive PDLA spherulite, respectively, that result from a reduction of the raw

Received: June 4, 2011
Published: August 12, 2011

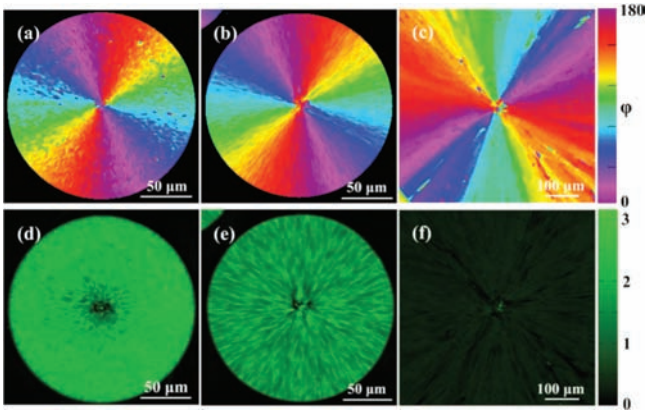

Figure 2. Extinction micrographs (λ = 630 nm) of optically negative (larger index tangential) PDLA (a) and PLLA (b) spherulites (thickness ~5 μm) and optically positive (larger index radial) PDLA spherulite (c). Angle is direction of large refractive index measured counterclockwise from the horizontal. (d–f) |LB| micrographs corresponding to (a–c) in radians.

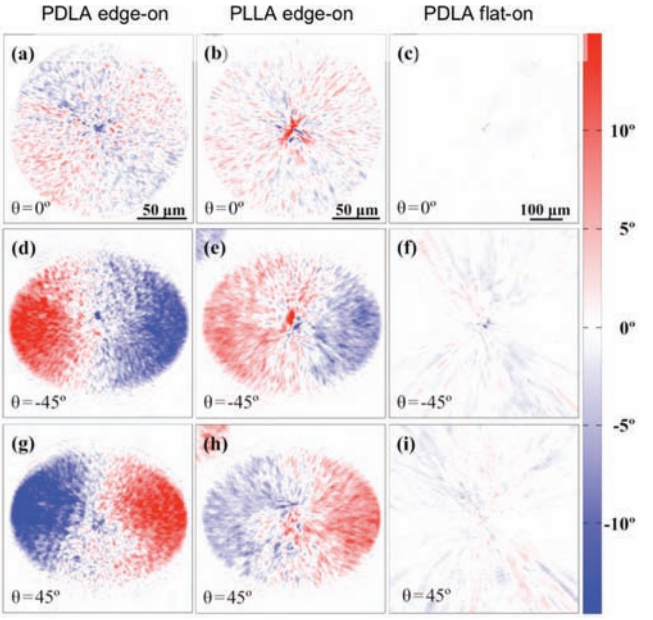

Figure 3. Circular birefringence (λ = 590 nm) of PLA spherulites. (a, d, g) PDLA edge-on spherulite in normal incidence, tilted at −45° and +45°, respectively. (b, e, h) PLLA edge-on spherulite in normal incidence, tilted at −45° and +45°, respectively. (c, f, i) PDLA flat-on spherulite in normal incidence, tilted at −45° and +45°, respectively.

M to false color micrographs representing discrete optical properties. The negative spherulites (edge-on lamellae) exhibited much stronger LB than the barely anisotropic positive spherulite (flat-on lamellae). This distinction results from the different spatial arrangements of lamellae. The chain stems are parallel to the substrate and perpendicular to the light in edge-on lamellae in normal incidence. They are perpendicular to the substrate and parallel to the incident light in flat-on lamellae. In the latter direction, the sample is nearly uniaxial. The organization of lamellae with respect to one another was expected from analysis of the CB micrographs. Figure 3 shows the CB signal of three radial spherulites. The spherulite consisting of flat-on lamellae hardly shows any CB (Figure 3c), and the spherulites consisting of edge-on lamellae (both PDLA and PLLA) exhibit a weak signal with an apparent random variation in sign (Figure 3a,b).

On tilting the samples about an axis perpendicular to the wave vector a large CB signal developed of opposite sign in the hemicircular regions separated by the plane parallel to the wave vector and perpendicular to the substrate and tilting axis. The sign of the signal was not correlated with the configuration of the monomers; PDLA and PLLA gave the same signal sense for a clockwise twist of the sample axis emerging on the left side when facing with the forward propagating beam (Figure 3d,e). However, a counterclockwise rotation of the sample changed the absolute signs of the CB signal for both enantiomers (Figure 3g,h).

Where does the CB come from? First, we will propose a qualitative model to account for the observations in broad strokes. Then, we will offer a quantitative simulation.

The expectation of CB is wholly consistent from a consideration of the symmetry of the experiment. Any two edge-on lamellae, originating from a spherulite nucleation center, but diverging radially in planes both normal to the substrate, comprise a C_{2v} crystalline ensemble, ignoring the fact that the lamellae are made from chiral molecules. Tilting occurs around the diad axis relating a pair lamellae. C_{2v} is an achiral but optically active point group;[14] dextro- and levorotatory directions in an oriented C_{2v} structure must be counterbalanced. The sign of the signal must change whenever the light vector is reflected across either of the two mirror planes. The observation of CB here is precisely what would be expected from our calculation of the optical activity of a single oriented water molecule[15] (Figure 4a) or the measurement of the CB of microwaves from a C_{2v} array of microfabricated U-shaped resonators likewise rotated about the diad axis (Figure 4b).[16]

The best explanation for optical activity often depends on the scale of the system. In H_2O, the optical activity arises, in large measure, from the non-normal transition electric dipoles and transition magnetic dipoles when projected onto the wavevectors of the light.[15] In the metamaterials, the CB arises from classical dipole moments induced in wires by electromagnetic radiation,[16] again with the proviso that, in an oriented system, the moments are not orthogonal on average with respect to the light beam. The symmetry of these experiments is analogous to PLA in Figure 4c. But, the origin of the polymer CB is best explained otherwise.

What is crucial for the observation of CB in PLA spherulites is the disposition of linearly birefringent lamellae, not molecular chirality. To account for the growth of the CB signal on tilting and its change in sign about the plane normal to the tilting axis, a reconsideration of the very first model of optical activity, Reusch's pile of twisted mica plates, is required.[17,18] Reusch recognized that he could mimic optical rotation in crystals by stacking flakes of mica each rotated in the same sense by a small amount from layer to layer. A circular wheel with radial, edge-on lamellae viewed in oblique incidence mimics a helical stack.

We could not affect a similar rise in CB when we tilted the spherulite with flat-on lamellae (Figure 3f,i). At first, one might expect that the edge-on and flat-on morphologies would have convergent optical properties at 45°. But, the flat-on lamellae are less well structured. The Bragg peaks are much coarser.[19] Additionally, the light path through the polymer, simply calculated from Snell's Law, is 28° with respect to the high birefringence direction in edge-on lamellae and 62° from the high birefringence direction in the flat-on lamellae. According to an approximate formula[20] for the Reusch stack, the azimuthal rotation is proportional to the square

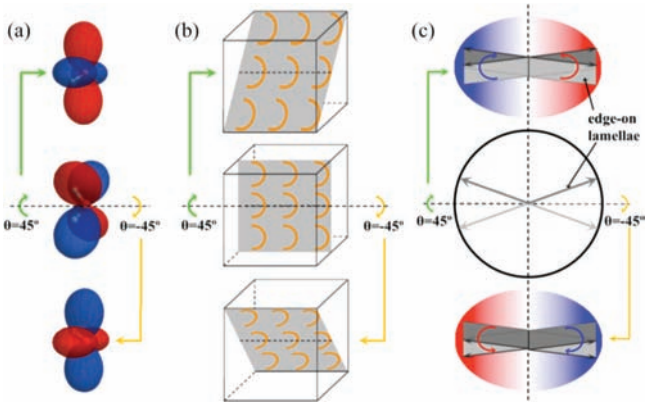

Figure 4. Circular birefringence determined by the sense of twisting of disparate C_{2v} objects. (a) Representation surface of optical rotation tensor of a single oriented water molecule at 45° (top), 0° (center) and −45° (bottom). (b) Split ring metamaterial resonators oriented likewise. (c) Representation of two PLA lamellae. Each half of the spherulite perpendicular to the twisting axis is a C_{2v} arrangement.

of the retardance. Together these factors account for the differences in the CB of edge-on and flat-on lamellae.

Symmetry arguments can tell us nothing about the magnitude of an effect. We therefore attempted to capture what is known about the structure of PLA spherulites in a quantitative model. Pockels[20] first derived an approximate formula for the azimuthal rotation expected from a pile of Reusch plates in normal incidence that was later supported by a more exact approach using the Jones calculus.[21] In order to deal with Reusch plates in non-normal incidence, we carried out the following calculation using the Stokes−Mueller calculus detailed in the Supporting Information. We estimated the refractive indices of a single PLA layer as 1.55 along the polymer chains and 1.45 and 1.46 in the orthogonal directions. According to AFM data, each layer was assumed to be 5 nm thick. The light path sampling a total thickness of t is pictured passing from layer to layer and interacting with the dielectric susceptibility tensor that is progressively mis-oriented as the light traverses the sample in non-normal incidence (Figure 5a−c). We assumed a misorientation of layers in the xy plane due to the radial orientation about z and in the yz plane due to the spherulitic growth mechanism. Then we took the general M of an anisotropic layer, taking out all the terms associated with diattenuation (absorption and dichroism) and intrinsic (molecular) CB. This M was multiplied by a succession of matrices each representing one layer with LB parameters evaluated from refractive indices derived from the rotated dielectric susceptibility tensor according to the physical disposition of layers as established. The experimental values in Figures 2d,e and 3d,e,g,h and the calculated values in Figure 5d,e compare favorably.

We know virtually nothing about the anisotropy of CB in high polymers with the exception of three reports on single crystals of PLA by Kobayashi,[22] the modern pioneer of the study of optically active crystals,[23] and co-workers. They reported an enormous and inordinately anisotropic CB: the components along and normal to the helical axes of the PLA chains were 9.2×10^3 °/mm and −14°/mm, respectively. This would be by far the largest OR in a crystal yet measured and the most anisotropic. On the other hand, the OR of glasses of PLLA were only 1.0−1.7°/mm at 25 °C,[23] values we confirmed by MM. The average of a very great value and two small values would still be quite large. The

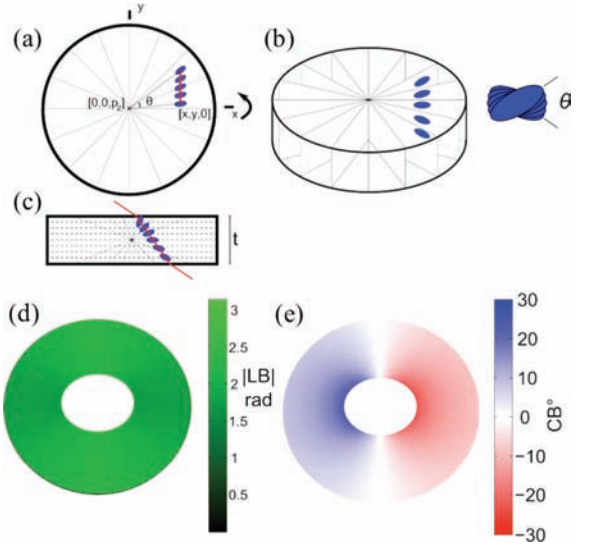

Figure 5. (a−c) Diagram showing oblique light path through a spherulite. (a) Normal to the spherulite. (b) Along the light path. (c) Perpendicular to the spherulite. As the light propagates through the material, the refractive index alignment rotates due to the inclined light path interacting with the radial structure. (d) The calculated |LB| in radians (λ = 590 nm) of a spherulite with principal refractive indices of [1.45,1.46,1.55] that was 8 μm thick with a diameter of 100 μm at an angle of incidence of −45° and numerically estimated with 20 layers. (e) Calculated CB (deg). The central regions in d,e have been obscured since the model in the very center becomes unphysical. Lamellae occupy the same space in the model at the core. The layers in the computation have a finite thickness. Moreover, the centers of the spherulites are typically less well organized. See AFM comparison in the Supporting Information.

discrepancy between glasses and crystals was explained by the earlier researchers on the basis of conformation selection boosting crystalline OR. In our polycrystalline PLA, we observed OR of ±3°/μm (Figure 3d,e,g,h) or $\pm 3 \times 10^3$ °/mm, comparable to the values for the ostensible single crystals. We thus conjecture that the PLA single crystals observed previously may not have been single but more likely twinned anisotropic lamellae with nonparallel extinction directions; the Bragg peaks in the wide-angle X-ray diffractograms showed considerable arcing.[24]

Authors commonly refer to 'natural optical activity' meaning CB or circular dichroism that is expressed by molecules dissolved in solution. This implies that there is a lesser, 'non-natural' optical activity that in the past we have described as artifactual.[7] Of course, what is normal or natural depends entirely on our experiences. Two centuries focused on isotropic media homogeneous along the light path have colored our outlook on optical activity. Based on our experience here, it is preferable to merely distinguish those systems that show CB from those that do not. The model one chooses to explain CB is a matter for individual investigators in particular circumstances. But, from an experimental point of view, it makes little sense to qualify CB as natural or otherwise. In principle, molecular and mesoscale CB can be separated with a more sensititve polarimeter based on photoelastic modulation currently under construction.

■ ASSOCIATED CONTENT

Supporting Information. Outline of optical model, Matlab implementation, and representative atomic force micrographs.

The material is available free of charge via the Internet at http://pubs.acs.org.

AUTHOR INFORMATION

Corresponding Author
jun-xu@mail.tsinghua.edu.cn; bart.kahr@nyu.edu

ACKNOWLEDGMENT

B.K. thanks the U.S. National Science Foundation (CHE-0845526) and the Petroleum Research Fund of the American Chemical Society for support of this research. J.X. is grateful to the Natural Science Foundation of China (No. 20974060) for financial support. We thank Dr. O. Arteaga for assistance in the implementation of his algorithm in ref 8.

REFERENCES

(1) Li, C. Y.; Cheng, S. Z. D.; Ge, J. J.; Bai, F.; Zhang, J. Z.; Mann, I. K.; Chien, L.-C.; Harris, F. W.; Lotz, B. *J. Am. Chem. Soc.* **2000**, *122*, 72–79. Li, C. Y.; Ge, J. J.; Bai, F.; Calhoun, B. H.; Harris, F. W.; Cheng, S. Z. D. *Macromolecules* **2001**, *34*, 3634–3641. Wang, J.; Li, C. Y.; Jin, S.; Weng, X.; Van Horn, R. M.; Graham, M. J.; Zhang, W.-B.; Jeong, K.-U.; Harris, F. W.; Lotz, B.; Cheng, S. Z. D. *Ind. Eng. Chem. Res.* **2010**, *49*, 11936–11947. Wang, J.-S.; Feng, X.-Q.; Xu, J.; Qin, Q.-H.; Yu, S.-W. *J. Comput. Theor. Nanosci.* **2011**, *8*, 1278–1287.

(2) Sélégny, E. *Optical Active Polymers*; D. Reidel: Dordrecht, 1979. Green, M. M.; Park, J.-W.; Sato, T.; Teramoto, A.; Lifson, S.; Selinger, R. L. B.; Selinger, J. V. *Angew. Chem., Int. Ed.* **1999**, *38*, 3138–3154.

(3) The Mueller matrix measurements were carried out on a home-made Mueller matrix microscope. It is constructed from an LED, a rotating optical diffusor, two linear polarizers (Thorlabs), two achromatic wave plate combinations (Thorlabs), a sample holder, and a Hamamatsu digital CCD. Further details are given in ref 7.

(4) Auras, R., Lim, L.-T., Selke, S. E. M., Tsuji, H., Eds. *Polylactic Acid*; Wiley: Hoboken, NJ, 2010.

(5) Domb, A. J.; Kumar, N.; Sheskin, T.; Bentolila, A.; Slager, J.; Teomim, T. *Polymeric Biomaterials*; Marcel Dekker: New York, 2001.

(6) Goldstein, D. H. *Polarized Light*, 2nd ed.; Marcel Dekker: New York, 2003.

(7) Freudenthal, J. H.; Hollis, E.; Kahr, B. *Chirality* **2009**, *21*, E20–E27.

(8) Arteaga, O.; Canillas, A. *J. Opt. Soc. Am. A* **2009**, *26*, 783–793.

(9) Arteaga, O.; Canillas, A.; Purrello, R.; Ribó, J. M. *Opt. Lett.* **2009**, *34*, 2177–2179. Freudenthal, J. H.; Hollis, E.; Kahr, B. *Chirality* **2009**, *21*, S20–S27. Arteaga, O.; Canillas, A.; Crusats, J.; El-Hachemi, Z.; Llorens, J.; Sacristan, E.; Ribo, J. M. *ChemPhysChem* **2010**, *11*, 3511–3516. Arteaga, O.; El-Hachemi, Z.; Canillas, A.; Ribó, J. M. *Thin Solid Films* **2011**, *519*, 2617–2623. Shtukenberg, A. G.; Freudenthal, J.; Kahr, B. *J. Am. Chem. Soc.* **2010**, *132*, 9341–9349.

(10) Poly(L-lactide) (PLLA) and poly(D-lactide) (PDLA) were kindly and freely provided by Purac Biomaterials. PLLA and PDLA have inherent viscosities of 2.56 and 2.40 dL/g, respectively, and were used without further purification.

(11) Sasaki, S.; Asakura, T. *Macromolecules* **2003**, *36*, 8385–8390.

(12) Xu, J.; Guo, B.-H.; Zhou, J.-J.; Li, L.; Wu, J.; Kowalczuk, M. *Polymer* **2005**, *46*, 9176–9185. He, Y.; Fan, Z.; Hu, Y.; Wu, T.; Wei, J.; Li, S. *Eur. Polym. J.* **2007**, *43*, 4431–4439. Wang, X.; Prud'homme, R. E. *Macromol. Chem. Phys.* **2011**, *212*, 691–698.

(13) The morphologies were observed with a polarized optical microscope (Olympus BX-50) equipped with a digital camera (Nikon D-80) and a first order red (530 nm) wave plate to establish optical sign.

(14) Claborn, K.; Isborn, C.; Kaminsky, W.; Kahr, B. *Angew. Chem., Int. Ed.* **2008**, *47*, 5706–5717.

(15) Isborn, C.; Claborn, K.; Kahr, B. *J. Phys. Chem. A* **2007**, *111*, 7800–7804.

(16) Plum, E.; Fedotov, V. A.; Zheludev, N. I. *J. Opt. A: Pure Appl. Opt.* **2009**, *11*, 074009.

(17) Reusch, E. *Ann. Phys. Chem.* **1869**, *138*, 628–638.

(18) Joly, G.; Billard, J. *J. Opt. (Paris)* **1981**, *12*, 323–329.

(19) Gazzano, M.; Focarete, M. L.; Riekel, C.; Scandola, M. *Biomacromolecules* **2004**, *5*, 553–558. See also: Kanchanasopa, M.; Manias, E.; Runt, J. *Biomacromolecules* **2003**, *4*, 1203–1213.

(20) Pockels, F. *Lehrbuch der Kristalloptic*; Teubner: Leipzig, 1906; pp 289−290.

(21) Jones, R. C. *J. Opt. Soc. Am.* **1941**, *31*, 500–503.

(22) Kobayashi, J.; Asahi, T.; Ichiki, M.; Oikawa, A.; Suzuki, H.; Watanabe, T.; Fukada, E.; Shikinami, Y. *J. Appl. Phys.* **1995**, *77*, 2957–2973. Kobayashi, J.; Asahi, T.; Ichiki, M.; Oikawa, A. *Ferroelectrics* **1995**, *171*, 69–94. Ichiki, M.; Asahi, T.; Kobayashi, J. *Phase Trans* **1996**, *5*, 67–78. The last report gives a different value of 3×10^4 °/mm for the most active direction.

(23) Kobayashi, J.; Uesu, Y. *J. Appl. Crystallogr.* **1983**, *16*, 204–211.

(24) Bratus, J.; Weng, D.; Vogl, O. *Polym. Int.* **1994**, *34*, 433–442. Goodman, M.; D'Alagni, M. *J. Polym. Sci., Part B: Polym. Lett.* **1967**, *5*, 515–521.

(25) Hoogsteen, W.; Postema, A. R.; Pennings, A. J.; G. ten Brinke, G. *Macrmolecules* **1990**, *23*, 634–642. See also:Montes de Oca, H.; Ward, I. M. *J. Polym. Sci., Part B: Polym. Phys.* **2007**, *45*, 892–902.

NOTE ADDED IN PROOF

According to a recent report (Wasanasuk, K.; Tashiro, K.; Hanesaka, M.; Ohhara, T.; Kurihara, K.; Kuroki, R.; Tamada, T.; Ozeki, T.; Kanamoto, T. *Macromol.* Articles ASAP, DOI: 10.1021/ma2006624) wide-angle X-ray diffraction data for PLLA is more consistent with the space group $P12_11$ rather than $P2_12_12_1$. This slight revision of the symmetry of the crystalline polymers studied here has no bearing on our results or conclusions.